Heliyon 10 (2024) e40125

Contents lists available at ScienceDirect

Heliyon

journal homepage: www.cell.com/heliyon

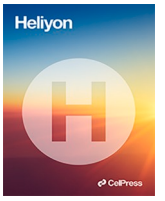

Research article

Evaluating constraints on offshore wind farm installation across the Taiwan Strait by exploring the influence of El Niño-Southern Oscillation on weather window assessment

Wan-Ling Tseng [a,b,*], Cheng-Wei Lin [b], Yi-Chi Wang [c], Huang-Hsiung Hsu [b], Kuan-Ming Chiu [d], Yueh-Shyuan Wu [e], Yi-Huan Hsieh [f,g], Ying-Ting Chen [b]

[a] Ocean Center, National Taiwan University, Taipei, Taiwan
[b] Research Center for Environmental Changes, Academia Sinica, Taipei, Taiwan
[c] Swedish Meteorological and Hydrological Institute, Sweden
[d] Department of Energy Engineering, Nation United University, Taiwan
[e] Green Energy and Environment Research Laboratories, Industrial Technology Research Institute, Hsinchu, Taipei, Taiwan
[f] Office of Sustainability, National Taiwan University, Taipei, Taiwan
[g] International Degree Program in Climate Change and Sustainable Development, National Taiwan University, Taipei, Taiwan

ARTICLE INFO

Keywords:
Offshore wind farm
ENSO
Taiwan Strait

ABSTRACT

The transition to renewable energy sources, such as offshore wind farms, is essential in mitigating climate change. Taiwan has set ambitious targets to harness wind energy from the Taiwan Strait, but offshore wind farm installations are highly dependent on weather conditions, particularly wind speeds. This study examines the relationship between the El Niño-Southern Oscillation (ENSO) and offshore wind farm installation by assessing weather windows—periods with wind speeds below 12 m per second at a height of 100 m for at least 12 h. Our analysis shows that during La Niña years, the number of feasible weather windows decreases by up to 40 %, particularly between October and June, compared to neutral and El Niño years. This decrease can be as high as fourfold in December, significantly impacting installation schedules. Seasonal variations are also notable, with wind speeds exceeding 12 m s^{-1} in winter 66.4 % of the time, compared to 29.4 % in spring, making spring and summer the most favorable periods for installation. However, even during these favorable seasons, La Niña years can bring higher wind speeds, necessitating careful planning. These results underscore the importance of integrating ENSO forecasts into project planning to avoid installation delays and optimize installation timelines. By leveraging seasonal and interannual climate variability predictions, decision-makers can improve the resilience of offshore wind farm projects and ensure efficient energy transition strategies.

1. Introduction

In pursuit the target of the 2050 net-zero emission of green-house gases in Paris Agreement, the Taiwanese government is grappling with the formidable task of transitioning its energy landscape. One of its official strategies involves the development of offshore wind

* Corresponding author. Ocean Center, National Taiwan University, Taipei, Taiwan.
E-mail address: wtseng@ntu.edu.tw (W.-L. Tseng).

https://doi.org/10.1016/j.heliyon.2024.e40125
Received 27 May 2024; Received in revised form 2 November 2024; Accepted 4 November 2024
Available online 5 November 2024

farms to harness renewable energy sources. The short-term objective is to generate 5.6 GW of energy by 2025, with a subsequent increase of 1.5 GW by 2030. In the long term, the ambitious goal is to reach a total capacity of 40∼55 GW by 2050 (https://www.ndc.gov.tw). The Taiwan Strait offers an advantageous geographical location with consistently strong mean wind speeds, making it an ideal setting for offshore wind farm development [1]. However, this advantage of heightened wind speeds also suggests a significant challenge to the progress of offshore wind farm projects. Excessive surface wind intensification can lead to project halts due to safety concerns. For operation purpose, the 'weather window' refers to conditions suitable for construction within a favorable wind environment. While the limited weather windows for operation, the huge mobilization cost of installation vessels, harsh environmental damage to equipment [2]. If inappropriate weather window conditions persist over the course of a year, it could result in construction delays, jeopardizing the achievement of both the short-term 2030 goal and the long-term 2050 objective.

Generally, offshore wind energy is closely associated with climate change [3] and climate variability [4]. Investigating the impact of wind intensity on offshore wind sites has been a focal area of research globally, with studies conducted in regions such as the Mediterranean Sea [5], Iranian islands [6], the Colombian Caribbean [4], and other areas [7,8]. In the Taiwan Strait, few studies have explored the impact of large-scale environmental factors on wind speed and wind energy production assessments. For instance Ref. [1], conducted a comprehensive review of the environmental conditions surrounding the first offshore wind farm case in the Taiwan Strait. Their findings revealed distinct seasonal patterns, with winter exhibiting the highest wind speeds and summer the lowest, consistent with the mean state wind circulation over Taiwan. Besides, the presence of a strong diurnal cycle, driven by land-sea breeze phenomena, resulted in a bimodal probability distribution. Tropical cyclones also play a significant role in contributing to extreme wind energy conditions in the region [9]. Furthermore, the impact of climate warming on wind energy density distributions has been evaluated, indicating a potential increase in the future, albeit with a slight 3 % reduction compared to past climate periods [10]. While most studies have focused on wind energy production, there remains a significant gap in the assessment of installation and maintenance aspects. In a limited literature review, it was observed that the annual number of feasible weather windows decreased as the window length increased, particularly in the Hsinchu compared to the Changhua surrounding sea region. Notably, November emerged as a more accessible month than adjacent winter months, primarily due to its correlation with lower wave heights. Paterson [11] highlighted the uncertainties associated with offshore installation, emphasizing that these uncertainties can lead to extended construction schedules and increased capital expenditure for projects. Given the critical importance of maritime meteorological risk assessments in the offshore wind industry, there is a notable lack of predictability in weather windows for installation at various time scales, from seasonal to decadal. To address this gap, it is imperative to explore the feasibility of wind speed assessments with reliable and accurate predictive information, which can provide valuable insights for decision-makers in the offshore wind sector.

In order to achieve this objective, several crucial steps must be taken. First and foremost, it is imperative to establish a robust link with environmental controls as predictive indicators, such as the El Niño-Southern Oscillation (ENSO). ENSO is a dominant and widely recognized climate variability phenomenon with significant implications for seasonal predictions [12]. ENSO patterns exhibit irregular but periodic oscillations, occurring approximately every two to seven years. These oscillations lead to predictable shifts in ocean surface temperatures and trigger a cascade of global climate effects. As a result, ENSO is often referred to as the heart of climate prediction worldwide [13]. It is particularly noteworthy for its influence on extreme weather events such as heavy rainfall and heatwaves. Given the critical role of ENSO in climate dynamics, studies on its impact on Taiwan have been extensive. Most of these investigations have focused on mainland Taiwan, emphasizing variations in rainfall [14–16] and temperature [17]. However, there has been relatively limited research dedicated to the Taiwan Strait region. Earlier work by Kuo and Ho [18] utilized satellite data to observe differences in sea surface wind patterns, identifying weaker winds during the 1997/1998 El Niño event and stronger winds during the 1998/1999 La Niña event. Subsequently, Ou, Zhai and Li [19] conducted a study that highlighted the impact of ENSO on wind patterns during the northeasterly monsoon seasons. The findings revealed that El Niño (La Niña) years led to weakened (strengthened) winds induced by lower-tropospheric anomalous anticyclones (cyclones) over the western Pacific Ocean and the South China Sea. However, a comprehensive, long-term statistical analysis of the relationship between ENSO and wind speed over the Taiwan Strait has been notably absent from previous research endeavors. This gap in knowledge has hindered the conversion of valuable insights into actionable information for stakeholders in the installation and operation of wind energy systems in the region.

The principal aim of this study is to establish a link between one of the most significant climate variability phenomena, ENSO, and its impact on wind speeds over the Taiwan Strait. Furthermore, the concept of a 'weather window', which is commonly employed in the offshore wind farm construction sector, will be employed as a relevant index. By establishing this connection, the current state of ENSO prediction can be utilized as a valuable resource for providing critical weather window information to decision-makers. This study makes a significant contribution to the existing literature by providing a comprehensive analysis of the influence of ENSO on wind speeds over the Taiwan Strait. The concept of weather windows for offshore wind farm installation is introduced, offering a practical tool for decision-makers in the offshore wind sector. The findings enhance understanding of seasonal and interannual variations in wind speeds and their implications for the planning and execution of offshore wind projects. Furthermore, the importance of integrating climate variability into renewable energy planning is highlighted, contributing to the development of more resilient and adaptive strategies for offshore wind farm installation and operation. The article is structured as follows: Section 2 provides an overview of the data and methodology employed in this study, while Section 3 shows the obtained results. The subsequent Section 4 delves into a comprehensive discussion of the findings.

2. Data and methodology

This section introduces the data used in this study, including environmental parameters and the ENSO index. It also defines the concept of the weather window and includes the validation of wind speed data.

2.1. Observed data

The large-scale atmospheric variables, such as surface 100-m winds, were obtained from the fifth generation of the European Centre for Medium-Range Weather Forecasts (ERA5), which was on a 0.25° × 0.25° grid from the period between 1980 and 2022 [20]. All the calculation is based on daily data. Climatology is defined as the period covering from 1980 to 2022. The seasonal definitions are as follows: winter includes December to February (DJF); spring encompasses March to May (MAM); summer covers June to August (JJA); and autumn spans September to November (SON). The aforementioned abbreviations can be verified in Table 1.

Two datasets are employed to evaluate the accuracy of ERA5 on the regional domain. Firstly, observed wind speed data from a wind tower situated at Waisanding Sand Bar (23.445811°N, 120.040911°E; depicted by the green cross in Fig. 2) in Chiayi City is utilized. This data is sourced from the Green Energy and Environment Research Laboratories at the Industrial Technology Research Institute through personal communication. The wind tower is located on one of the largest sandbars in southwest Taiwan to study realistic near-surface offshore wind variations at a height of 60 m. The available data spans from January 2007 to September 2022. Hourly data is retrieved and converted from locate time (UTC+8 Taipei time) to UTC by applying an 8-h shift to facilitate comparison with ERA5. Secondly, the regional reanalysis data is also examined by the Meteorological-Information Based Green Energy Operations Center, Center Weather Agency (CWA) in Taiwan (https://greenmet.cwa.gov.tw) hereafter referred to as the CWA Green Energy Data. These datasets are developed in Taiwan for green energy assessment, real-time monitoring, forecasting, and offshore wind farm installation systems. The data is generated using CWA/WRF with a horizontal resolution of 3 km, covering the period from 2018 to 2022. The variable of interest in this comparison is wind speed at a height of 100 m. To facilitate comparison with ERA5, the data is regridded to a resolution of 0.25°.

The Oceanic Niño Index (ONI) is selected as the primary ENSO index for this study and is retrieved from the Climate Prediction Center website (https://origin.cpc.ncep.noaa.gov/products/analysis_monitoring/ensostuff/ONI_v5.php). The ONI represents the rolling 3-month average temperature anomaly in the surface waters of the east-central tropical Pacific, near the International Dateline (5°N-5°S, 120°-170°W). The months are labeled using the middle month of the 3-month period. Additionally, a 30-year base period is applied every 5 years. Index values of +0.5 or higher indicate El Niño, while values of −0.5 or lower indicate La Niña.

2.2. Definition of weather window

The duration of operations and maintenance activities at offshore wind farms is contingent upon surface wind conditions that allow for the safe access of vessels to wind turbines. Moreover, one of the primary economic factors influencing capital expenditure during installation is downtime caused by unfavorable weather windows [21]. Consequently, gaining insights into weather windows is imperative when planning operational activities. A weather window refers to a period during which both wind speed and wave height remain below specified thresholds for a minimum continuous duration. These thresholds dictate when vessels can access wind turbines to conduct specific maintenance tasks. Various operation and maintenance strategies are employed for different weather windows to ensure the optimal availability of wind turbines. As outlined in the previous study [22], the specific thresholds for wind speed vary for distinct maintenance operations, ranging from 8 to 20 m s^{-1} at a height of 100 m. For this assessment, the reference threshold selects 12 m s^{-1} continuous persistent longer than 12 h to calculate the weather window. The offshore wind farm locations selected for this study is from 24°N to 24.5°N and from 119.75°E to 120.25°E, which align with the primary target for completion by 2030 (https://sites.google.com/view/t-wind-marine-association, Fig. 1).

2.3. Wind speed data validation

To conduct a thorough analysis of the ENSO effect, it is essential to utilize extensive, high-quality data over a large domain. ERA5 provides wind speed data with excellent temporal and spatial resolution, making it ideal for this purpose. In contrast, the CWA Green Energy Data, which incorporates dynamic downscaling, provides reliable regional assessments of wind fields. However, its six-year dataset may not be sufficient to fully capture ENSO variability. To validate the representativeness of ERA5 data, we compared it with observed wind speeds from an observed wind tower and CWA Green Energy Data (Fig. 2). To quantify the accuracy of ERA5 against CWA Green Energy Data, we used Pearson correlation coefficients, mean absolute error (MAE), and skill scores for pattern evaluation. The Pearson correlation R is defined as [23]:

Table 1
Abbreviation table.

Abbreviations	Descriptions
CWA	Center Weather Agency in Taiwan
DJF	December, January, and February
ENSO	El Niño-Southern Oscillation
ERA5	Fifth generation of the European Centre for Medium-Range Weather Forecasts
JJA	June, July and August
MAM	March, April and May
ONI	Oceanic Niño Index
SON	September, October and November

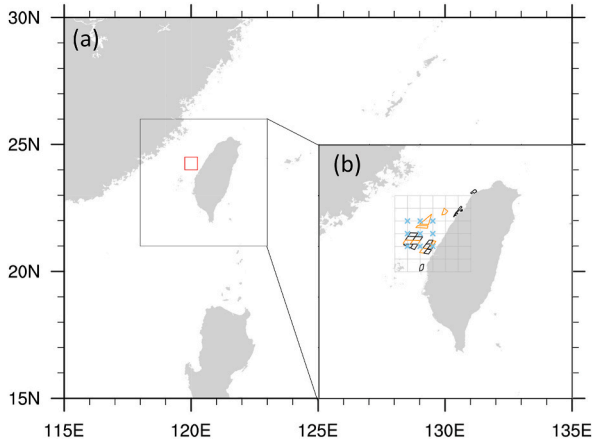

Fig. 1. The current wind farms that are operational, under construction, and potential locations within two domains: (a) the larger East Asia domain and (b) the specific Taiwan regional domain. In this depiction, the installed wind turbines are denoted by black irregular boxes, while areas under construction are shown by orange boxes. The focal point of our assessment lies within the blue cross domain, spanning coordinates 24°N to 24.5°N and 119.75°E to 120.25°E, which has been selected as the primary offshore wind farm location for our study.

$$R = \frac{\sum_i (x_i - \bar{x})(y_i - \bar{y})}{\sqrt{\sum_i (x_i - \bar{x})^2 \sum_i (y_i - \bar{y})^2}} \tag{1}$$

where x_i and y_i are the ERA5 and CWA Green Energy Data, respectively. The MAE is calculated as:

$$MAE = \frac{\sum_1^n |y_i - x_i|}{n} \tag{2}$$

where n is the number of time steps. The skill score S is calculated as [24]:

$$S = \frac{4(1+R)}{\left(\sigma + \frac{1}{\sigma}\right)^2 (1+R_0)} \tag{3}$$

where R represents the spatial pattern correlation coefficient between ERA5 and CWA Green Energy Data, and σ is the ratio of the spatial standard deviation of ERA5 relative to CWA Green Energy Data. R_0 is the maximum correlation attainable, which is assumed to be 1 in this case.

The evaluation metrics for wind speed, comparing ERA5 data with CWA Green Energy Data and observed wind tower data are shown in Fig. 2. The correlation map (Fig. 2a) between ERA5 and CWA Green Energy Data indicates an overall correlation value exceeding 0.9 over the Taiwan Strait, affirming its reliability. Furthermore, comparison with observed wind tower data reveals a correlation of 0.92, demonstrating realistic wind speed variations even against actual observed data. Moreover, when extending the observed data to 16 years, the correlation values remain robust in terms of wind speed (Fig. 2b). Consequently, ERA5 emerges as a dependable data source for our analysis. Over the wind farm region, the MAE values range from 1 to 2 m s^{-1}, with larger biases observed closer to the coastline (Fig. 2c). These higher errors near the coast likely stem from the complex interactions between land and sea, which can create more challenging conditions for accurate wind speed modeling. Despite these biases, the skill scores remain within the range of 0.8–0.9 (Fig. 2d), indicating that ERA5 data maintains strong reliability. A skill score of 1 represents a perfect match between datasets, while lower values indicate weaker agreement; the relatively high skill scores thus confirm ERA5's dependable performance in capturing wind speed patterns. This metrics evaluates the performance of ERA5 wind speed data by comparing it with CWA Green Energy Data and wind tower observations using metrics such as correlation coefficients, MAE, and skill scores. The results suggest that ERA5 is a reliable data source for assessing offshore wind speeds, particularly in open ocean regions, making it well-suited for evaluating offshore wind farm potential.

3. Results

This section first provides a diagnostic analysis of the mean state and ENSO circulation. It then examines the impact of ENSO on wind speed assessments. Finally, the results of the weather window detection are investigated.

3.1. Mean states and El Niño-Southern Oscillation circulation

The mean-state circulation over the Taiwan Strait is primarily influenced by the East Asian monsoon [25]. Fig. 3 demonstrates the

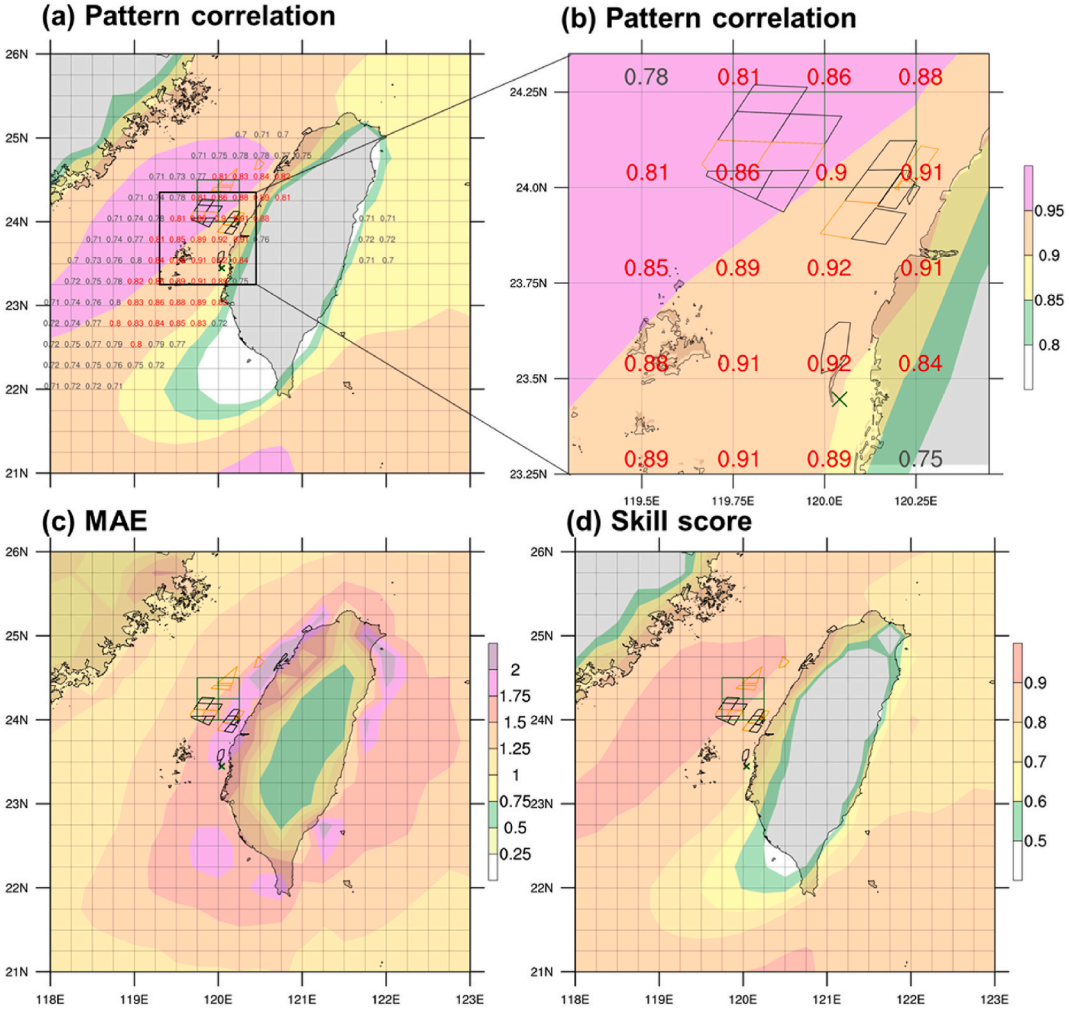

Fig. 2. Evaluation metrics of the wind speed. (a) Shading indicates the correlation coefficient between ERA5 and CWA Green Energy Data. The numbers indicate the correlation of ERA5 with the observed wind tower data (green cross). Red colors indicate correlations higher than 0.8. The daily averaged data is from 2018 to 2022, spanning six years. (b) Similar to (a) but with a smaller domain outlined by the black box in (a) and using longer period from 2007 to 2022, covering 16 years for textual information. Missing data from the wind tower is excluded from all calculations. (c) Shading shows the Mean Absolute Error (MAE) between ERA5 and CWA Green Energy Data. (d) Shading represents skill scores between ERA5 and CWA Green Energy Data. A skill score of 1 indicates an identical match between the two datasets.

circulation climatology and ENSO composite of winter and summer season. During the winter monsoon season, the strong Siberian high-pressure system, situated in Siberia and the Mongolian Plateau, directs cold and dry winds toward the warmer and moister regions of East and Southeast Asia (Fig. 3a). This extensive continental climate system results in a robust northeasterly wind pattern along the western boundary of the Pacific Ocean, which then turns east-northeasterly as it crosses the Taiwan Strait (climatology). However, during El Niño years, a distinct cyclonic circulation pattern materializes over the northwest Pacific (Fig. 3b), offsetting the typical south-westerly anomaly and consequently leading to a reduction in wind speeds. In contrast, La Niña years produce conditions conducive to cyclonic circulation over the western Pacific, resulting in a north-easterly anomaly that amplifies the background wind speed (Fig. 3c). During the East Asian summer monsoon, a converse circulation pattern emerges, characterized by the prevalence of robust southerly winds across the Taiwan Strait (Fig. 3d). Notably, during El Niño summers, a cyclonic circulation configuration takes shape over the northwest Pacific, contributing to the weakening of the southerly mean flow (Fig. 3e), while La Niña summers foster southerly intensification, partly attributed to the presence of an anticyclone situated east of Taiwan and the Philippines (Fig. 3f). While the winter season prominently exhibits the ENSO-associated circulation signals, the summer season showcases a comparatively less pronounced response to ENSO.

Delving into the seasonal dynamics, the correlation between wind speed and the ONI index from 1980 to 2022 is shown in Fig. 4. As previously mentioned, the ONI index represents the rolling 3-month average temperature anomaly in the surface waters of the tropical Pacific. The months are labeled using the middle month of each 3-month period. The shading in the figure represents the correlation coefficients between the ONI index and 100-m wind speed across various regions. The color bar on the right indicates the strength of

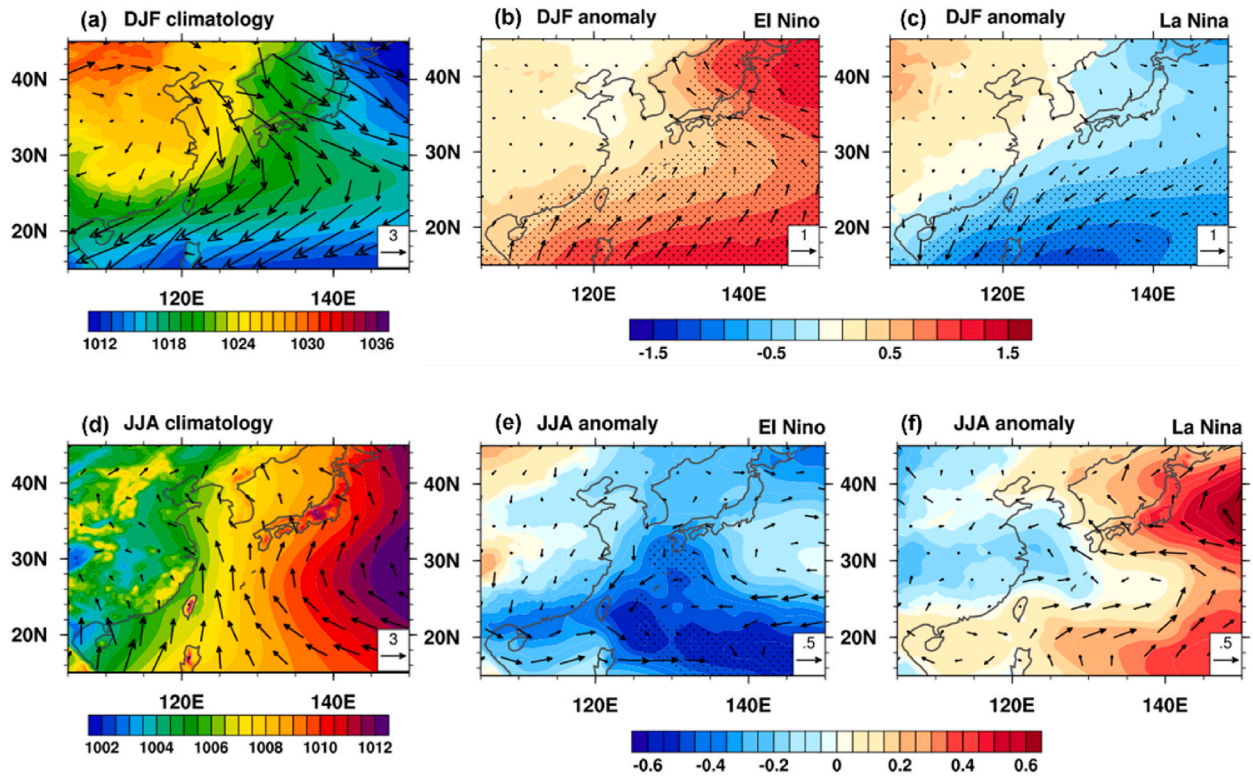

Fig. 3. The sea level pressure climatology and ENSO anomalous sea level pressure (shading; hPa) along with 850 hPa wind (vectors; m s-1) over East Asia. The top row [(a–c)] corresponds to the winter season, while the bottom row [(d–f)] corresponds to summer. Panels (a), (d) represent the climatology, panels (b), (e) show El Niño conditions, and panels (c), (f) display La Niña conditions. Dots on the figure indicate significance levels at the 90 % confidence level.

these correlations: positive values suggest a direct relationship (i.e., higher wind speeds during El Niño events), while negative values indicate an inverse relationship (i.e., higher wind speeds during La Niña events). This is especially relevant for offshore wind farm installations, as changes in wind speed due to ENSO can significantly impact operations. The black dots in the figure represent regions where the correlations are significant at the 99 % confidence level. The correlation strength varies across the region, with some areas showing stronger positive or negative correlations, highlighting that ENSO's influence on wind speeds is not uniform. Most months exhibit a negative correlation over the Taiwan Strait, suggesting weaker winds during El Niño events and stronger winds during La Niña events. September is the sole exception, showing a weak positive correlation. The extensive significant areas in the figure demonstrate that ENSO has a statistically significant influence on wind speeds across a wide region. Notably, the significant negative correlation is particularly pronounced from October to May, indicating consistently weaker winds during El Niño years and stronger winds during La Niña years during winter seasons. In conclusion, Fig. 4 demonstrates the substantial impact of ENSO on wind speeds in the Taiwan Strait region, with statistically significant patterns. This information is crucial for optimizing wind farm operations and planning, particularly during La Niña years when wind speeds tend to be higher.

3.2. Impact of El Niño-Southern Oscillation on wind speed assessments

While evaluating the offshore wind farm locations as depicted in Fig. 1, the probability distribution of wind speed ratios, averaged across the installation domain, is shown in Fig. 5. In alignment with the broader circulation patterns, this seasonal analysis reveals a bimodal probability distribution characterized by higher wind speeds in winter and lower speeds in summer. The threshold for transitioning from weak to strong winds is set at 12 m s^{-1}. The distribution of wind speeds over the entire year ranks as follows: DJF (66.4 %), SON (52.4 %), MAM (29.4 %), and lastly JJA (15.4 %). It is worth noting that from spring to summer, conditions are more favorable for offshore wind turbine installation.

The straightforward relationship between ENSO and wind speed over the offshore wind farm is illustrated in Fig. 6a, where the right axis represents 100-m wind speed anomalies (m/s). These anomalies are calculated by subtracting the monthly climatology, allowing for a focus on deviations from the average wind conditions. The strong negative correlation of −0.56 supports the previous conclusion that El Niño tends to weaken wind speeds, while La Niña years strengthen them, generally speaking. However, an unexpected pattern emerges when the probability distribution of wind speeds during ENSO events (Fig. 6b) is examined in closer detail. The ratio of wind speeds exceeding 12 m s^{-1} is actually higher during La Niña years (34.7 %) compared to El Niño years (29.9 %), with the

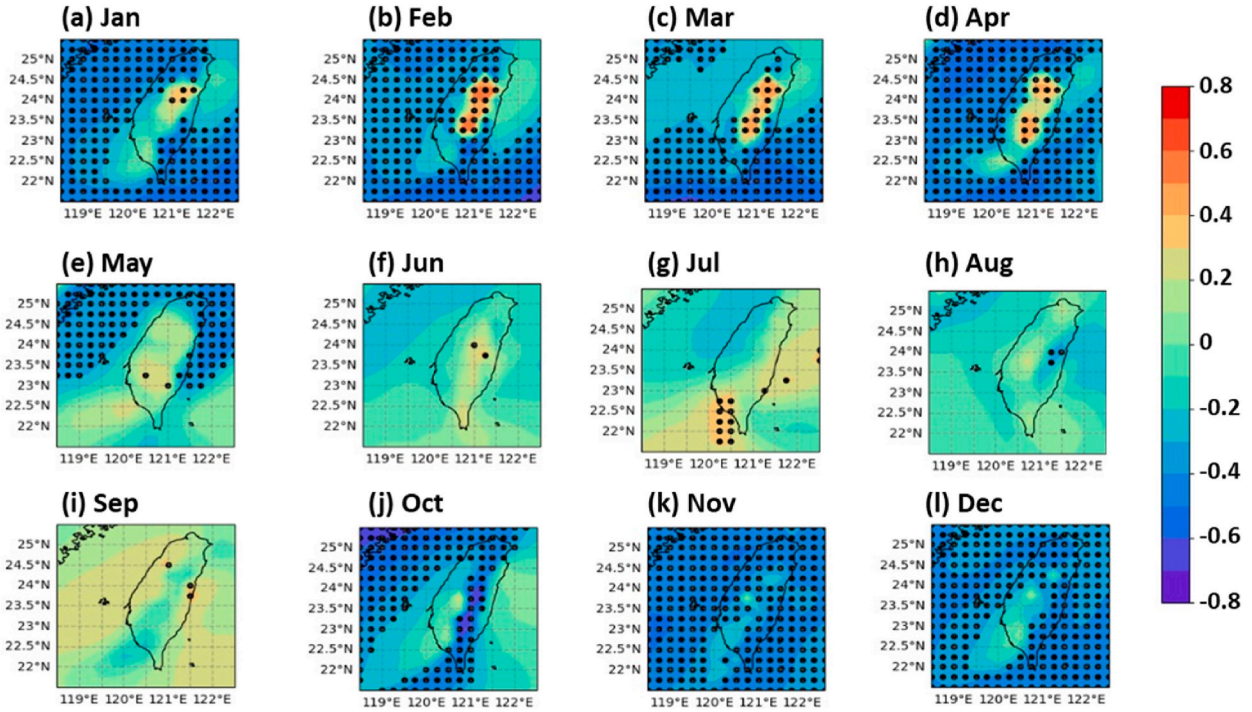

Fig. 4. Correlation between the ONI index and 100-m wind speed. The shading represents the correlation coefficients between the ONI index and 100-m wind speed across various regions. The color bar on the right indicates the strength and direction of the correlations. Dots on the figure represent regions where the correlations are significant at the 99 % confidence level.

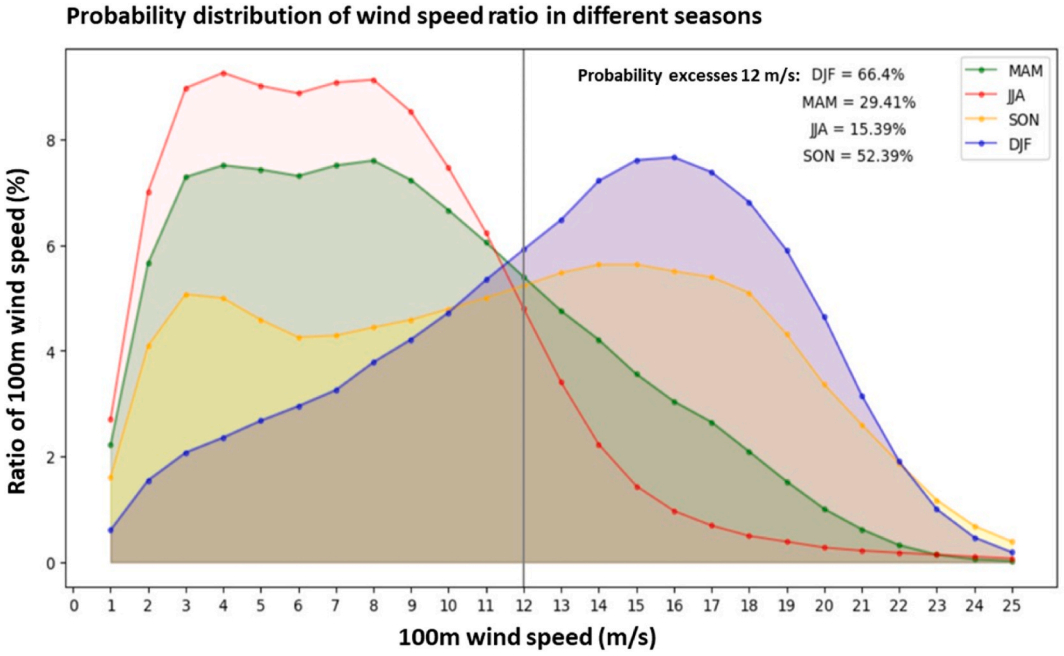

Fig. 5. The probability distribution function of 100-m wind speed associated for different seasons. The figure displays the probability distribution function (PDF) of 100-m wind speeds for the four seasons: MAM (spring), JJA (summer), SON (autumn), and DJF (winter). The vertical line marks the 12 m s^{-1} threshold, with the percentage values indicating the probability of exceeding this wind speed in each season. DJF (winter) has the highest probability of wind speeds exceeding 12 m s^{-1} (66.4 %), followed by SON (52.39 %), MAM (29.41 %), and JJA (15.39 %).

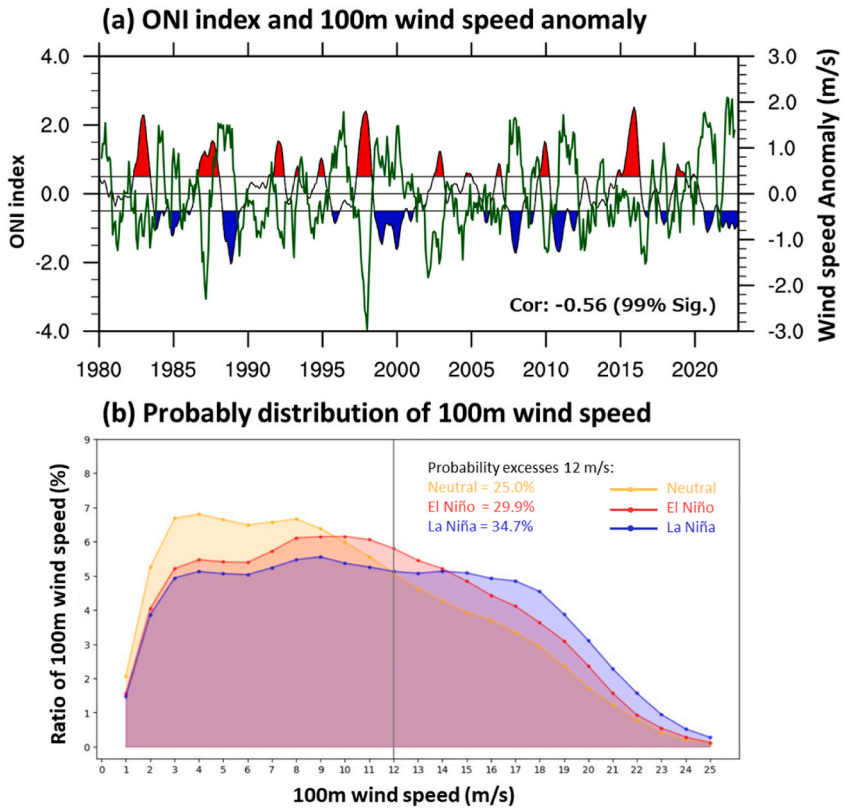

Fig. 6. Relationship between ENSO and wind speed. (a) On the left axis, it shows the ONI index, and on the right axis, it displays the 100-m wind speed anomalies (m s^{-1}) averaged over the region in the Taiwan Strait (as outlined by the yellow box in Fig. 1b). Anomalies are calculated by removing the monthly climatology to highlight deviations from the norm. (b) The panel displays the probability distribution function of 100-m wind speed for neutral (yellow), El Niño (red), and La Niña (blue) events.

lowest ratio occurring in neutral years (25 %). Interestingly, neutral years have a mean wind speed position in between but tend to have a left-skewed distribution. This implies that not only do La Niña years impact installation progress negatively, but El Niño years also have a secondary adverse effect.

The box plots in Fig. 7 provide a more detailed view of wind speeds for each season. In principle, the spring and summer seasons are more favorable for wind turbine installation due to the generally lower wind speeds that fall below the threshold of 12 m s^{-1}. During these seasons, particularly in La Niña years, there is a higher likelihood of encountering favorable wind conditions that facilitate installation activities. Conversely, the autumn and winter seasons show greater challenges, with a higher probability of winds exceeding 12 m s^{-1}, especially during La Niña years. This pattern highlights the considerable impact of the ENSO signal, which is most pronounced during the winter season, resulting in stronger winds that can impede installation efforts. The analysis indicates that while spring offers the most optimal conditions for installation, it is essential to implement meticulous planning and adaptive strategies to mitigate the adverse effects of ENSO, particularly during the autumn and winter months. It is also noteworthy that interannual variability is investigated, as shown in Fig. 8. It is not surprising that during autumn and winter, La Niña years exhibit the highest frequency of wind speeds exceeding 12 m s^{-1}. However, neutral years contribute more to this condition than El Niño years. This variability indicates that even in the absence of a strong ENSO signal, wind speeds can still pose significant challenges during neutral years. It is noteworthy that when wind power generation is considered instead of installation, La Niña years also show challenging conditions, characterised by numerous minimum peaks during the summer season. This suggests that La Niña impacts not only the installation windows but also the operational efficiency of wind farms during the summer months, necessitating comprehensive planning for both installation and operational phases.

3.3. Detection of weather window

To align with the objectives of the installation assessments, wind speed data is transformed into weather window information to facilitate the co-production of climate services. As outlined in Section 2, the weather window criteria entail wind speeds below 12 m s^{-1} at a height of 100 m and a duration of at least 12 h. The total count of feasible weather windows is visualized in Fig. 9, revealing significant variability throughout the year, with occurrences ranging from 12 to 56. La Niña conditions lead to a notable reduction in workable weather windows, particularly from October to June. This reduction is most pronounced during the winter and spring

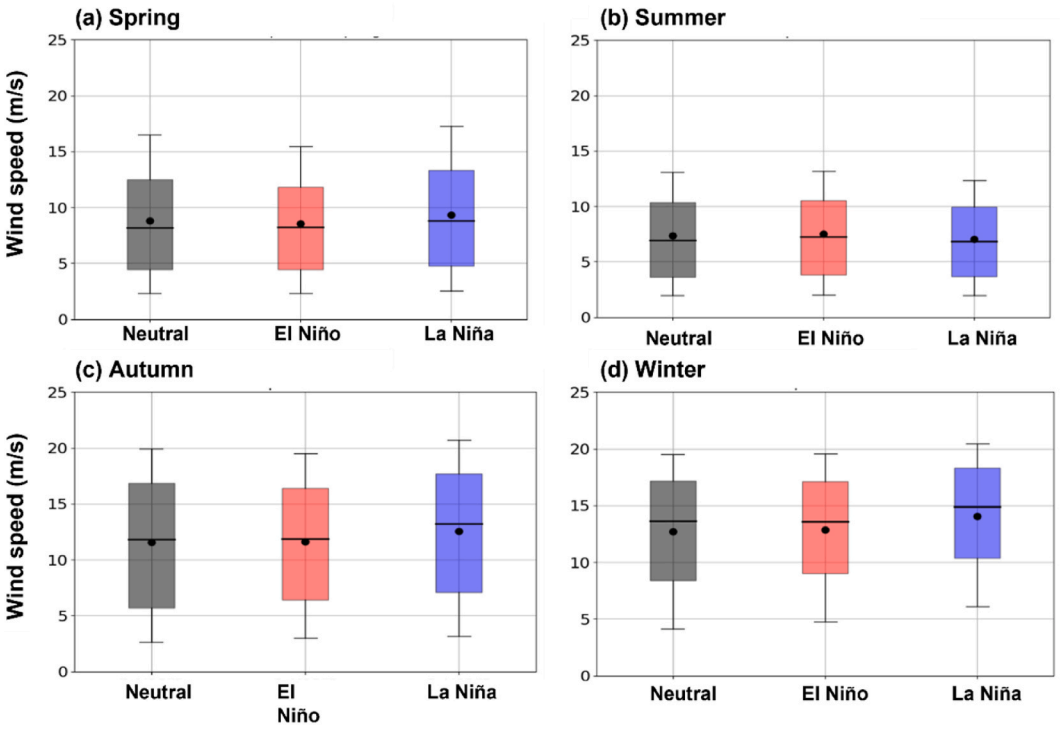

Fig. 7. Box plots of wind speed in each season. (a) Spring, (b) Summer, (c) Autumn, and (d) Winter. The box plots represent the distribution of 100-m wind speeds during each season, with the central black dot indicating the mean wind speed. The whiskers represent the range of wind speeds, and the interquartile range (IQR) is depicted by the boxes. The plots compare neutral (gray), El Niño (red), and La Niña (blue) phases, highlighting seasonal variations and the influence of ENSO on wind speeds.

months when the strong ENSO signal impacts wind patterns, resulting in fewer opportunities for safe and efficient wind turbine installation. Conversely, El Niño and neutral conditions offer more stable and favorable weather windows, especially during the summer and early autumn months, when the number of feasible weather windows peaks. The chart shows that during La Niña years, the number of workable weather windows decreases significantly during the late autumn and winter months, reaching its lowest in December. This decrease highlights the challenges posed by stronger wind conditions associated with La Niña events, which can impede installation activities. In contrast, the number of weather windows increases during the spring and summer months under neutral and El Niño conditions, providing more opportunities for installation during these periods. To provide precise quantification, supplementary data detailing weather window statistics relative to climatology for each month from 1980 to 2022 is included. This data supports the identification of optimal periods for installation and helps in planning and decision-making processes. By understanding the monthly and seasonal distribution of weather windows, stakeholders can better anticipate and mitigate the impacts of ENSO on offshore wind farm installations, ensuring more efficient and resilient project execution.

Additionally, Fig. 10 illustrates the anomalies in weather window occurrences. During extreme months, such as December, weather windows can decrease by up to fourfold during La Niña years, while they may increase by up to fivefold in November during El Niño years. This figure shows the monthly anomalies of weather windows under different ENSO conditions, providing a clear representation of how ENSO phases can significantly alter the availability of suitable installation periods. In January, La Niña conditions show a significant decrease in weather windows (an anomaly of −3.1), while El Niño conditions show a moderate increase (an anomaly of 1.5). This trend continues in February, with La Niña showing a decrease (−2.6) and El Niño an increase (1.5). The pattern reverses in the spring and summer months, where La Niña conditions generally show increased weather windows, such as in July (an anomaly of 2.6), while El Niño conditions often show decreases, particularly in July (−2.8) and August (−2.1). These anomalies highlight the complexity and variability introduced by ENSO events. La Niña tends to reduce the number of weather windows during critical installation months in late autumn and winter, while El Niño can provide more favorable conditions during these periods. Understanding these anomalies is crucial for optimizing installation schedules and ensuring efficient resource allocation. By analyzing these seasonal and interannual variations, stakeholders can better anticipate and manage the risks associated with offshore wind farm installations. This comprehensive understanding of weather window anomalies under different ENSO conditions allows for more informed decision-making, ensuring that installation activities are planned during the most favorable periods and adapting strategies to mitigate the adverse effects of ENSO.

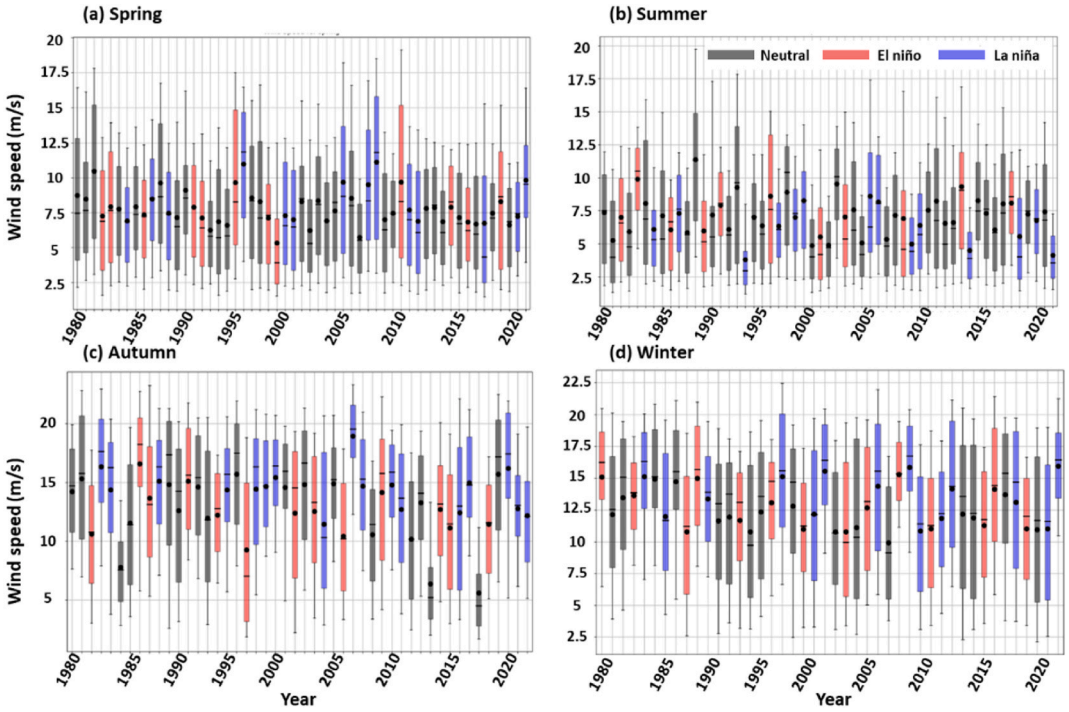

Fig. 8. Box plots of interannual wind speed in each season from 1980 to 2022. (a) Spring, (b) Summer, (c) Autumn and (d) Winter. The box plots display the interannual variability of 100-m wind speeds for each season over the period from 1980 to 2022. The data is categorized by ENSO phase: Neutral (gray), El Niño (red), and La Niña (blue). The boxes represent the interquartile range (IQR), the whiskers indicate the range of wind speeds, and the black dots represent the mean wind speed for each year.

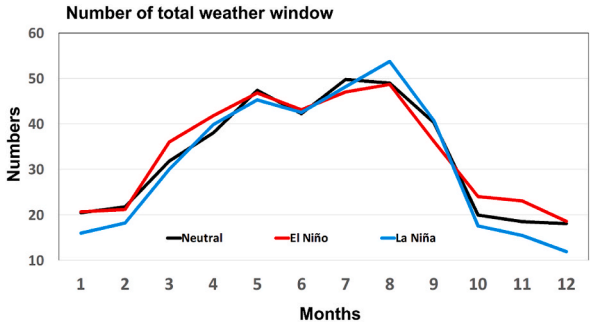

Fig. 9. Number of total weather windows in neutral (black), El Niño (red), and La Niña (blue) events. The figure shows the total number of weather windows across each month for Neutral (black), El Niño (red), and La Niña (blue) events. The x-axis represents the months of the year, while the y-axis indicates the number of available weather windows.

4. Discussion

This study investigates the impact of the ENSO on offshore wind farm installation assessments in the Taiwan Strait, with a primary focus on evaluating the suitability of weather windows for installation. Weather conditions significantly influence the installation process, and understanding the correlation between ENSO events and wind speeds is critical. The study utilizes the ONI to establish this correlation, defining weather windows based on a threshold wind speed of 12 m s^{-1} at a height of 100 m. The analysis covers four seasons: winter, spring, summer, and autumn.

The study reveals a strong negative correlation between ENSO and wind speed over the Taiwan Strait. El Niño events tend to result in weaker wind speeds, while La Niña events strengthen wind speeds. This relationship is crucial for predicting installation windows and planning accordingly. However, a detailed examination of wind speed probability distributions during ENSO events brings surprising insights. Contrary to expectations, wind speeds exceeding 12 m s^{-1} occur more frequently during La Niña years (34.7 %) than El Niño years (29.9 %), with neutral years falling in between (25 %). This indicates that even neutral years, which do not have strong ENSO signals, can still significantly impact installation progress.

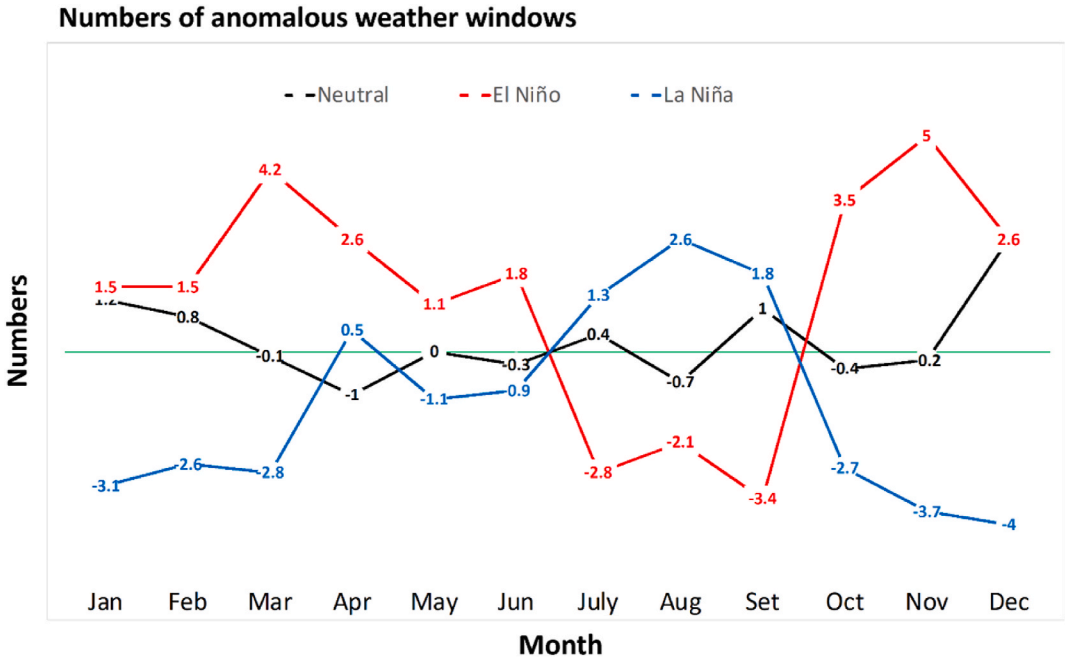

Fig. 10. Number of anomalous weather windows in neutral (black), El Niño (red), and La Niña (blue) events. The figure illustrates the monthly anomalies in the number of weather windows for Neutral (black), El Niño (red), and La Niña (blue) phases. The x-axis represents the months of the year, and the y-axis shows the deviation from the average number of weather windows, with positive values indicating more weather windows than the average and negative values indicating fewer.

Further analysis considers both seasonal and interannual variability. Spring and summer emerge as better seasons for installation, with higher possibilities of workable weather windows due to generally lower wind speeds. In these seasons, particularly during La Niña years, there is a higher likelihood of encountering favorable wind conditions that facilitate installation activities. Conversely, autumn and winter show greater challenges for installation, with higher probabilities of winds exceeding 12 m s^{-1}, particularly during La Niña years. This pattern underscores the substantial impact of the ENSO signal, which is most pronounced during the winter season, resulting in stronger winds that can impede installation efforts. Interannual variability reveals that La Niña years exhibit the highest frequency of wind speeds exceeding 12 m s^{-1} in autumn and winter. Neutral years also contribute significantly to high wind speed occurrences, while El Niño years show lower frequencies. Interestingly, when focusing on wind power generation instead of installation, La Niña years demonstrate challenges during the summer, characterized by numerous minimum peaks. This suggests that La Niña impacts not only installation windows but also the operational efficiency of wind farms.

Weather windows, defined by wind speeds below 12 m s^{-1} for at least 12 h, are critical for the safe and efficient installation of offshore wind turbines. The total count of feasible weather windows reveals significant variability throughout the year, with occurrences ranging from 12 to 56. La Niña conditions lead to a notable reduction in workable weather windows, particularly from October to June. This reduction is most pronounced during the winter and spring months when the strong ENSO signal impacts wind patterns. Conversely, El Niño and neutral conditions offer more stable and favorable weather windows, especially during the summer and early autumn months. The monthly anomalies of weather windows under different ENSO conditions further illustrate the impact. During extreme months, such as December, weather windows can decrease by up to fourfold during La Niña years, while they may increase by up to fivefold in November during El Niño years. This variability highlights the importance of considering ENSO phases in installation planning.

While wind conditions are critical for offshore wind farm installation, wave conditions are equally important in determining suitable weather windows. High wave heights and long wave periods can disrupt installation activities, pose risks to vessel operations, and cause significant project delays. Although this study focuses solely on 100-m wind speeds for evaluating weather windows, wave information is also crucial for assessing construction risks. Compared to wind data, wave characteristics—including height, frequency, and direction—are often more influential but come with greater uncertainty. Even in observational datasets, wave measurements are frequently obstructed or incomplete. In model data, high-resolution wind-wave modeling is typically required to capture wave behavior accurately. Therefore, an integrated approach that considers both wind and wave conditions is essential for accurately determining weather windows and mitigating risks. Future studies should aim to combine wave data with wind speed assessments to provide a more comprehensive framework for offshore wind farm planning and operations.

Despite the challenges posed by environmental impacts on offshore wind farm installation being mentioned in previous studies [1,2,9], a comprehensive investigation covering the entire wind farm sector in Taiwan has not been thoroughly conducted [4]. Most existing studies focus on the impact of climate warming [3] on wind energy generation, with limited attention given to installation

risks. This gap in research makes it difficult for decision-makers to develop near-term policies, particularly in the context of Taiwan's 2050 net-zero target. This study uses Taiwan and ENSO's impact as a case study to demonstrate that assessing interannual climate variability is crucial for near-term future risk assessments. The findings highlight the importance of incorporating climate variability into global wind farm installation assessments [4–6], emphasizing the need for more detailed evaluations to inform future energy policy and planning.

5. Conclusion

In this research, the ENSO is selected as the indicator to evaluate interannual wind speed variability. The advantage of using ENSO is that it is one of the dominant drivers of interannual variability, with a pronounced and well-documented signal. Additionally, ENSO typically provides good predictability in state-of-the-art seasonal prediction models, offering valuable information for decision-makers. However, the disadvantage is that ENSO is not the only factor influencing wind speed variability, and relying solely on it may overlook other important climatic factors. Thus, while ENSO provides a robust framework for predictions, it should be integrated with other indicators for a more comprehensive assessment. The key conclusion of this studies.

(1) Impact of ENSO on Wind Speeds: ENSO significantly influences wind speeds in the Taiwan Strait, with El Niño events leading to weaker winds and La Niña events resulting in stronger winds, especially during the winter months.
(2) Seasonal and Interannual Variability: Spring and summer are identified as the most favorable seasons for offshore wind turbine installation, but La Niña years create challenges with increased wind speeds, particularly in autumn and winter.
(3) Reduction in Weather Windows: During La Niña years, the number of feasible weather windows decreases by up to 40 %, especially from October to June, making installation more difficult. In contrast, El Niño and neutral conditions offer more stable weather windows.

The findings from this study have several critical implications for offshore wind farm projects.

(1) By understanding the seasonal and interannual variations in wind speeds and weather windows, stakeholders can better anticipate favorable conditions for installation, ensuring efficient and resilient project execution.
(2) Quantifying the impact of ENSO events on weather windows contributes to the development of predictive tools and climate services that assist decision-makers in optimizing installation timing and resource allocation.
(3) The study's insights into the relationship between ENSO events and wind power generation underscore the need for comprehensive planning for both installation and operational phases.

Overall, this research improves our understanding of the complex interactions between climate variability and offshore wind energy projects, providing valuable insights for the sustainable development of renewable energy in the Taiwan Strait. Through seasonal forecasting, it is possible to effectively predict the scheduling of work vessels and the allocation of worker hours, thus optimizing the management of annual working hours. By using ENSO forecasts, decision-makers can better anticipate favorable conditions, ensure that installation activities are scheduled during optimal periods, and adjust strategies to mitigate the adverse effects of ENSO and long-term scheduling.

CRediT authorship contribution statement

Wan-Ling Tseng: Writing – review & editing, Writing – original draft, Validation, Supervision, Resources, Project administration, Methodology, Investigation. **Cheng-Wei Lin:** Visualization, Methodology, Formal analysis, Data curation, Conceptualization. **Yi-Chi Wang:** Writing – review & editing, Supervision, Conceptualization. **Huang-Hsiung Hsu:** Writing – review & editing, Supervision, Funding acquisition, Conceptualization. **Kuan-Ming Chiu:** Visualization, Formal analysis. **Yueh-Shyuan Wu:** Funding acquisition, Conceptualization. **Yi-Huan Hsieh:** Funding acquisition, Conceptualization. **Ying-Ting Chen:** Visualization, Methodology.

Data availability statement

The ERA5 data used in this study can be accessed from the ECMWF website at https://www.ecmwf.int/en/forecasts/dataset/ecmwf-reanalysis-v5. The weather window data is provided in the supplementary materials. Additional datasets generated and analyzed during the study are available from the first author upon request.

Declaration of competing interest

The authors declare that they have no known competing financial interests or personal relationships that could have appeared to influence the work reported in this paper.

Acknowledgments

This study was supported by the Industrial Technology Research Institute in Taiwan of project "Collection of offshore

meteorological observation, satellite, and reanalysis data in Taiwan and the Asia-Pacific region". Additional funding was provided by the Taiwan National Science and Technology Council under Grant, Taiwan (NSTC 113-2111-M-002-016 -, NSTC 112-2923-M-001-003-MY4). We are grateful to the National Center for High-Performance Computing for providing computer facilities. We thank to Industrial Technology Research Institute and Meteorological-Information Based Green Energy Operations Center, Center Weather Agency, Taiwan for providing the wind datasets.

Appendix A. Supplementary data

Supplementary data to this article can be found online at https://doi.org/10.1016/j.heliyon.2024.e40125.

References

[1] K.-S. Cheng, C.-Y. Ho, J.-H. Teng, Wind characteristics in the Taiwan Strait: a case study of the first offshore wind farm in taiwan, Energies 13 (2020) 6492.
[2] E. Barlow, D.T. Öztürk, M. Revie, E. Boulougouris, A.H. Day, K. Akartunalı, Exploring the impact of innovative developments to the installation process for an offshore wind farm, Ocean Engineering 109 (2015) 623–634.
[3] C.-w. Zheng, C.-t. Yi, C. Shen, D.-c. Yu, X.-l. Wang, Y. Wang, W.-k. Zhang, Y. Wei, Y.-g. Chen, W. Li, A positive climatic trend in the global offshore wind power, Front. Energy Res. 10 (2022) 867642.
[4] M. Bastidas-Salamanca, J.G. Rueda-Bayona, Effect of climate variability events over the Colombian caribbean offshore wind resource, Water 13 (2021) 3150.
[5] A. Martinez, G. Iglesias, Evaluation of offshore wind energy zones within marine spatial planning: a case study in the Spanish Mediterranean Sea, Energy Rep. 11 (2024) 3461–3473.
[6] M. Majidi Nezhad, M. Neshat, G. Piras, D. Astiaso Garcia, Sites exploring prioritisation of offshore wind energy potential and mapping for wind farms installation: Iranian islands case studies, Renew. Sustain. Energy Rev. 168 (2022) 112791.
[7] S. Hoseinzadeh, B. Nastasi, D. Groppi, D. Astiaso Garcia, Exploring the penetration of renewable energy at increasing the boundaries of the urban energy system – the PRISMI plus toolkit application to Monachil, Spain, Sustain. Energy Technol. Assessments 54 (2022) 102908.
[8] Q. Xu, Y. Li, Y. Cheng, X. Ye, Z. Zhang, Impacts of climate oscillation on offshore wind resources in China seas, Rem. Sens. 14 (2022) 1879.
[9] T.-Y. Lee, Y.-T. Wu, M.-T. Kueh, C.-Y. Lin, Y.-Y. Lin, Y.-F. Sheng, Impacts of offshore wind farms on the atmospheric environment over Taiwan Strait during an extreme weather typhoon event, Sci. Rep. 12 (2022) 823.
[10] T.-J. Chang, C.-L. Chen, Y.-L. Tu, H.-T. Yeh, Y.-T. Wu, Evaluation of the climate change impact on wind resources in Taiwan Strait, Energy Convers. Manag. 95 (2015) 435–445.
[11] J. Paterson, Metocean Risk Analysis in Offshore Wind Installation, 2019.
[12] M.J. McPhaden, S.E. Zebiak, M.H. Glantz, ENSO as an integrating concept in earth science, Science 314 (2006) 1740–1745.
[13] M. Latif, D. Anderson, T. Barnett, M. Cane, R. Kleeman, A. Leetmaa, J. O'Brien, A. Rosati, E. Schneider, A review of the predictability and prediction of ENSO, J. Geophys. Res.: Oceans 103 (1998) 14375–14393.
[14] J.-M. Chen, T. Li, C.-F. Shih, Asymmetry of the El niño-spring rainfall relationship in taiwan, Journal of the Meteorological Society of Japan. Ser. II 86 (2008) 297–312.
[15] Z. Jiang, G.T.-J. Chen, M.-C. Wu, Large-scale circulation patterns associated with heavy spring rain events over Taiwan in strong ENSO and non-ENSO years, Mon. Weather Rev. 131 (2003) 1769–1782.
[16] C.-C. Lin, Y.-J. Liou, S.-J. Huang, Impacts of two-type ENSO on rainfall over Taiwan, Adv. Meteorol. 2015 (2015).
[17] Y.c. Wu, J.L. Chu, Y.C. Yu, Climatology and the interannual variability of the high-temperature extremes in taiwan, J. Geophys. Res. Atmos. 125 (2020) e2019JD030992.
[18] N.J. Kuo, C.R. Ho, ENSO effect on the sea surface wind and sea surface temperature in the Taiwan Strait, Geophys. Res. Lett. 31 (2004).
[19] Y. Ou, F. Zhai, P. Li, Interannual wave climate variability in the Taiwan Strait and its relationship to ENSO events, Journal of Oceanology and Limnology 36 (2018) 2110–2129.
[20] H. Hersbach, B. Bell, P. Berrisford, S. Hirahara, A. Horányi, J. Muñoz-Sabater, J. Nicolas, C. Peubey, R. Radu, D. Schepers, The ERA5 global reanalysis, Q. J. R. Meteorol. Soc. 146 (2020) 1999–2049.
[21] R.T. Walker, L. Johanning, R. Parkinson, Weather windows for device deployment at UK test sites: availability and cost implications, in: Proceedings of the 9th European Wave and Tidal Energy Conference, 2011, pp. 5–9. Southampton, UK.
[22] J.-H. Liu, Study on the Weather Impact of the Installation Schedule of Offshore Wind Farm Turbines in the Taiwan Strait, Department of Civil Engineering National Taiwan University, 2019.
[23] D.S. Wilks, Statistical Methods in the Atmospheric Sciences, Academic press, 2011.
[24] K.E. Taylor, Summarizing multiple aspects of model performance in a single diagram, Journal of geophysical research: atmospheres 106 (2001) 7183–7192.
[25] B. Wang, The Asian Monsoon, Springer Science & Business Media, 2006.